INTERNATIONAL JOURNAL OF CLIMATOLOGY
Int. J. Climatol. **32**: 983–994 (2012)
Published online 7 April 2011 in Wiley Online Library
(wileyonlinelibrary.com) DOI: 10.1002/joc.2326

RMetS
Royal Meteorological Society

Four-dimensional structures and physical process of the decadal abrupt changes of the northern extratropical ocean–atmosphere system in the 1980s

Dong Xiao,[a] Jianping Li[b]* and Ping Zhao[c]

[a] *Chinese Academy of Meteorological Sciences, Beijing 100081, China*
[b] *National Key Laboratory of Numerical Modeling for Atmospheric Sciences and Geophysical Fluid Dynamics, Institute of Atmospheric Physics, Chinese Academy of Science, Beijing 100029, China*
[c] *National Meteorological Information Centre, Beijing 100081, China*

ABSTRACT: The four-dimensional structures and possible physical process of the decadal abrupt changes (DACs) of the northern extratropical ocean–atmosphere system in 1983–1988 are investigated by using ERSST.v2 and NCEP/NCAR reanalysis data. The DACs of sea surface temperature (SST) appeared over the southern tropical Atlantic, middle Pacific, and northern midlatitude oceans in 1983–1988. The atmospheric DACs in 1983–1988 were characterized with lower and higher geopotential height and air temperature anomalies over the Arctic and northern midlatitude, respectively. The above atmospheric distributions are attributed by the mass removal between the Arctic and middle latitudes. The decadal anomalies of the Ferrel cells and meridional atmospheric mass exchanges between the northern midlatitude and Arctic were suggestive of the DAC of the Northern Hemisphere annular mode (NAM).

Basing on the disclosed facts above, the possible physical process of the DACs in the 1980s is proposed as follows. The DACs of the northern midlatitude SST heated the lower tropospheric atmosphere and it made the meridional gradient of air temperature anomalies increase between the middle and high latitudes. Decadal anomalous Ferrel cell was triggered, which presented a meridional vertical current over the northern extratropics. The results of the meridional mass exchanges induced the lower geopotential height and air temperature over the Arctic, and higher ones over the northern midlatitude. In conclusion, the warming of the northern midlatitude SST may be responsible for the northern extratropical atmospheric DACs and associated climate change events in the 1980s. Copyright © 2011 Royal Meteorological Society

KEY WORDS decadal abrupt changes; four-dimensional structures; Ferrel cell; Northern Hemisphere annular mode; meridional atmospheric mass exchange

Received 17 October 2009; Revised 15 February 2011; Accepted 15 February 2011

1. Introduction

The decadal-multidecadal climate variability affects the lives of several billion people via its long-lived effects on agriculture, water resources, fisheries, and public health, even some social events (Mehta *et al*., 2000). The decadal climate variability is an important fluctuation for the century-scale climate changes. Therefore, the study of decadal climate variability is very important to confirm and predict global warming. Accordingly, the study of the decade-to-century-scale climate variability has been highlighted much more by the Climate Variability and Predictability (CLIVAR). The original studies on the DecCen climate variability focus on the structures and physical process over the North Pacific and North Atlantic (e.g. Nitta and Yamada, 1989; Trenberth, 1990; Deser and Blackman, 1993; Graham, 1994; Kushnir, 1994; Trenberth and Hurrell, 1994). Hence, the CLIVAR program stresses the importance of the characteristics and physical process of the decadal-multidecadal variability of the ocean–atmosphere system.

At present, the most striking decadal abrupt change (DAC, is defined as the abrupt transition from one stable state of mean value to another one within decade-to-century scale) around 1976 attracts much attention (e.g. Nitta and Yamada, 1989; Trenberth, 1990; Latif and Barnett, 1994; Trenberth and Hurrell, 1994; Mantua *et al*., 1997; Zhang *et al*., 1997; Deser *et al*., 2004; Yu and Zhou, 2007). The atmospheric DACs in the late 1970s happened over the tropics at all levels (Xiao and Li, 2007a). However, recent studies, as follow, presented the new DACs in the Northern Hemisphere (NH) extratropics in the 1980s, which is temporally and spatially independent of that in the 1970s. The characteristics of the DACs in the 1980s of oceanic, sea ice, and atmospheric systems were disclosed in terms of changes of warmer winter sea surface temperature (SST) in the northern North Pacific (Xiao and Li, 2007a); reduction in summer sea ice in the offshore region of Siberia (Maslanik *et al*., 1996) and the southern Okhotsk

* Correspondence to: Jianping Li, National Key Laboratory of Atmospheric Sciences and Geophysical Fluid Dynamics (LASG), Institute of Atmospheric Physics (IAP), Chinese Academy of Sciences (CAS), Beijing 100029, China. E-mail: ljp@lasg.iap.ac.cn

Sea (Tachibana *et al*., 1996); lower sea level pressure over the Arctic (Walsh *et al*., 1996), stronger North Atlantic Oscillation (NAO) (Watanabe and Nitta, 1999; Schwing *et al*., 2003), warmer spring over the Arctic (Overland *et al*., 2004) and Eurasia (Ting *et al*., 1996; Watanabe and Nitta, 1998), weaker winter subtropical jet streams over the North Pacific and North Atlantic Oceans (Ting *et al*., 1996; Watanabe and Nitta, 1998), stronger winter Siberia High and less occurrences of spring dust storms over northwest China (Ding *et al*., 2005; Liu and Ding, 2007; Zhu *et al*., 2008). Moreover, the DACs in the 1980s influenced the epipelagic ecosystems in the North Pacific (Hare and Mantua, 2000). Lo and Hsu (2010) suggested that the abrupt warming over the northern extratropics was associated with the influence of the Pacific Decadal Oscillation-like pattern and the Arctic Oscillation-like pattern. The northern extratropical DACs in the 1980s were identified by the above facts. Considering that the occurring time of the DACs may not be simultaneous in different regions and levels, we aim to investigate the four-dimensional structures and the possible physical process of the DACs of the northern extratropical ocean–atmosphere system in the 1980s. This study indicates that the northern extratropical atmospheric DACs in the 1980s may be caused by the DACs of northern midlatitudinal SST.

This study is organized as follows. The data and methodology are introduced in the next section. The horizontal, vertical, and temporal characteristics are investigated in Section 3. Decadal anomalies of meridional mass exchange between the northern middle and high latitudes, and their relationship to the NH annular mode (NAM) are explored in Section 4. In Section 5, the possible physical process is proposed and used to explain the associated climate change events. The summary and conclusion are in the last section.

2. Data and methodology

2.1. Dataset

In this study, we employ the annual averaged data, which are derived from the monthly datasets as follow. Monthly mean sea level pressure (SLP), upward long-wave radiation flux (ULWRF), surface air temperature (SAT), horizontal, vertical winds, and geopotential height fields in this study are obtained from the National Centers for Environmental Prediction/National Center for Atmosphere Research (NCEP/NCAR) reanalysis datasets (Jan. 1948–Feb. 2009) (Kalnay *et al*., 1996) on 2.5×2.5 degree latitude/longitude grid. The monthly mean extended reconstruction SST (ERSST.v2) (Jan. 1948–Feb. 2009) (Smith and Reynolds, 2004) is obtained from National Ocean and Atmosphere Administration (NOAA). The resolution is $2.0^\circ \times 2.0^\circ$. The results in this study are robust with the HadISST.v1 and European Centre for Medium-Range Weather Forecast (ECMWF) reanalysis data and the ERSST.v2 and NCEP/NCAR reanalysis data. Therefore, the data of greater length (NCEP/NCAR) were used in this study.

The annual index of the NAM (1873–2007) defined by Li and Wang (2003) is adapted in this study. The NAM index defined by Li and Wang (2003) is simply the difference in surface pressure between 35°N and 65°N around the hemisphere based on NCEP/NCAR monthly reanalysis data. Angell (2006) noted that this simple NAM index has a more symmetric correlation with surface pressure anomalies around the hemisphere than does the leading empirical orthogonal function of Thompson and Wallace (1998) and Wallace (2000).

2.2. Method

This study focused on decadal climate variability, the concepts of which are introduced here. Decadal climate variability is the climatic variability within decade-to-century time scales that is restricted by the time scales, but not by variational styles. Decadal climate variability may be divided into three types of variational styles (Martinson *et al*., 1995; Xiao and Li, 2007b). First, the period variation contains the decadal time scale period. Second, abrupt change stands for the rapid transition from one stable state to another. Under the different definitions for a stable state, abrupt change may be divided into abrupt change of mean value, variance, trend, probability and so on. Third, the gradual variation or decadal trend of climate variability indicates the slow transition between two stable states. Decadal abrupt change (namely, DAC) means rapid transition from one stable state to another one both within decade-to-century scale.

Jiang and You (1996) indicated that moving t-test technique (MTT) could detect the DAC years (DACYs, defined in the next paragraph) in a time series more than once, with a certain timescale. The MTT is used to detect abrupt change via examining whether the difference between the mean values of two sub-samples is significant or not. For a time series of the length n (X_i, $i = 1, 2, \ldots, n$), a certain sample is selected, by moving, as a cutting point to obtain the two subsets (x_1 and x_2) before and after it.

The t-statistic is defined as:

$$t = \frac{\overline{x}_2 - \overline{x}_1}{s.\sqrt{\frac{1}{n_1} + \frac{1}{n_2}}},$$

where $s = \sqrt{\frac{n_1 s_1^2 + n_2 s_2^2}{n_1 + n_2 - 2}}$, n_1, n_2 are the sub-sample sizes, namely, the detecting scales of MTT, $\overline{x}_1$, $\overline{x}_2$ are the mean values, and s_1^2, s_2^2 are the variances for the two subsets, respectively. Given a significant level α, the DACYs, viz., the DAC points, are named corresponding to the wave crests or troughs of the periods ($|t| \geq t_\alpha$) of t-statistic.

The presupposition of MTT is that the time series follows the normal distribution and the samples are independent each other. The DACYs are weighted by the

normal distribution of both sub-series of t-test warranted by the skewness and kurtosis test (Huang, 2000) at the 99% confidence level. The samples of the atmospheric and oceanic time series are generally not independent of each other. The effective degrees of freedom of t-test are expediently evaluated by the autocorrelation coefficient of the time series (Jiang *et al*., 2001). We employ MTT to detect the DACs in each time series in a field of ocean–atmosphere system. The horizontal and vertical distributions of the DACs of ocean–atmosphere system contain multiple testing problems that some DACs in a field might be false positive. Therefore, the Benjamini and Hochberg multiple testing correction (Benjamini and Hochberg, 1995) is adapted in this study to control the false discovery rate of the DACs in each field at 0.05. The more detailed introduction of MTT should be referenced in section 2.1 and 3 in Xiao and Li (2007a).

This paper focuses on decadal abrupt changes of mean value (DACMV, hereafter referred as DAC for simplicity). We take the detecting scales $n_1 = n_2 = 10$, a decadal time scale. The head and the tail of the time series are expanded 10 years with the beginning value and the ending value, respectively, so that we could capture all the DACYs in the data period. Presumed that there are m DACYs in a time series, the time series is divided into $m + 1$ episodes. The persistence time of each episode lasts equal to or more than the minimum of the detecting scales, maybe except the marginal ones. Each DACY in the time series is significant by t-test with the new detecting scales until no modification, which are the persistence time of the episodes before and after the DACY.

The MTT is employed to detect the DACYs of each time series of the oceanic and atmospheric variables. The horizontal and vertical distribution of the DACYs of the oceanic and atmospheric variables could be displayed by overlapping the time cross-section of the DACYs in the DAC event.

Epoch composite difference is used to show the decadal changes of the horizontal and vertical circulations before and after the DACYs. The choice of the epoch is illuminated in the footnote (*).

[*] The choice of the periods adopted in the epoch difference maps of Figure 6 and 7 are illuminated in this section. As noted above, the DACs of the 500-hPa geopotential height of West Canada occurred in 1984. Therefore, the epoch difference was disclosed before and after 1984. Xiao and Li (2007a) disclosed that atmospheric DACs occurred over the tropics and along the West America mainly in 1976. The latter period of the epoch difference analysis in Figure 6a is adopted the years 1985–1997, because the DACs of the Arctic geopotential height happened in 1997. However, the time series of 500-hPa geopotential height over the West Canada decreased after 1993 (Figure 3e), which may be influenced by the volcanic eruption of the Pinatubo Mountain on June 12–16, 1991 because the tropical and subtropical tropospheric temperature descended after it in several years (Self *et al*., 1998). In order to avoid the influences from the former DACs in 1976 and that from the volcanic eruption in early 1990s, the epoch difference of Figure 6a is adopted as 1985–1993 minus 1977–1984. The distribution of 1985–2004 minus 1965–1984 are similar to, but not significant than, that of 1985–1993 minus 1977–1984. The choices of the periods for the others panels of Figure 6 and Figure 7 are similar to that of Figure 6a.

3. Four-dimensional structures of the DACs of the ocean-atmosphere system in the 1980s

The horizontal distributions of the DACYs (in Figure 1) mean the occurrence times of the DACs of different regions. The vertical distributions of the DACYs (in Figure 3) refer to the occurrence times of the DACs of different levels of certain selected regions. The DAC episode, which is not the experience time of the transition of averaged state of a time series, is a period within the minimum of the detecting scales of MTT (a decade in this study) from the beginning to the ending of the DACs event (such as the DACs in the 1980s). Each DAC increases/decreases abruptly after the DACY. The DAC episode of the atmosphere-ocean system in the 1980s is from 1983 to 1988.

3.1. Horizontal distributions of the DACYs in the 1980s

Figure 1 shows the distributions of the DACYs of SST, upward long-wave radiation flux (ULWRF), SAT, SLP, 850-hPa, and 500-hPa geopotential height. The increased DACs (IDACs, the mean value of variable increases after the DACY) of SST (Figure 1(a)) occurred in the southern tropical Atlantic in 1983, in the eastern North Pacific in 1984, in the central North Atlantic in 1984–1985, in the middle Pacific in 1985, along the coast of west Europe in 1985–1987, and in the northern North Pacific in 1988. The DACs of ULWRF which indicated the decadal anomalous oceanic heating to the atmosphere took place over the southern tropical Atlantic, northern midlatitudal ocean, South Pacific and middle Indian Ocean (Figure 1(b)). The IDACs of SAT (Figure 1(c)) happened over northeast Asia in 1985, 1987–1988, over west Canada in 1985 and over north Europe in 1987. The decreased DACs (DDACs, the mean value of variable decreases after the DACY) of SAT occurred dispersedly over the Southern Hemisphere (SH) in 1987–1988. Figure 1(d) depicts that the decreased DACs (DDACs, the variable decreases after the DACY) of SLP took place over the Arctic in 1985–1987, over West Africa in 1986–1987 and over the SH circumpolar regions in 1984–1988. The IDACs of 500-hPa geopotential height (Figure 1(f)) happened over west Canada and northern subtropical Atlantic in 1984–1985, over East Asia in 1985–1988, and over west Europe in 1985–1987. The DDACs of 500-hPa geopotential height occurred over the Arctic in 1985 and 1987. In summary, the atmospheric structures of the DACs in the 1980s were generally characterized with the midlatitude IDACs and Arctic DDACs of geopotential height. The horizontal distributions of above variables showed that the DACYs of different regions and levels were not simultaneous.

Figure 2 shows the epoch difference maps of the NH 500-hPa geopotential height, 850-hPa air temperature and horizontal winds for forward-minus-later annual mean: 1986–1997 minus 1977–1985 and 1988–1997 minus 1977–1987, in view of the facts that the DACs of 500-hPa geopotential height and 850-hPa air temperature over

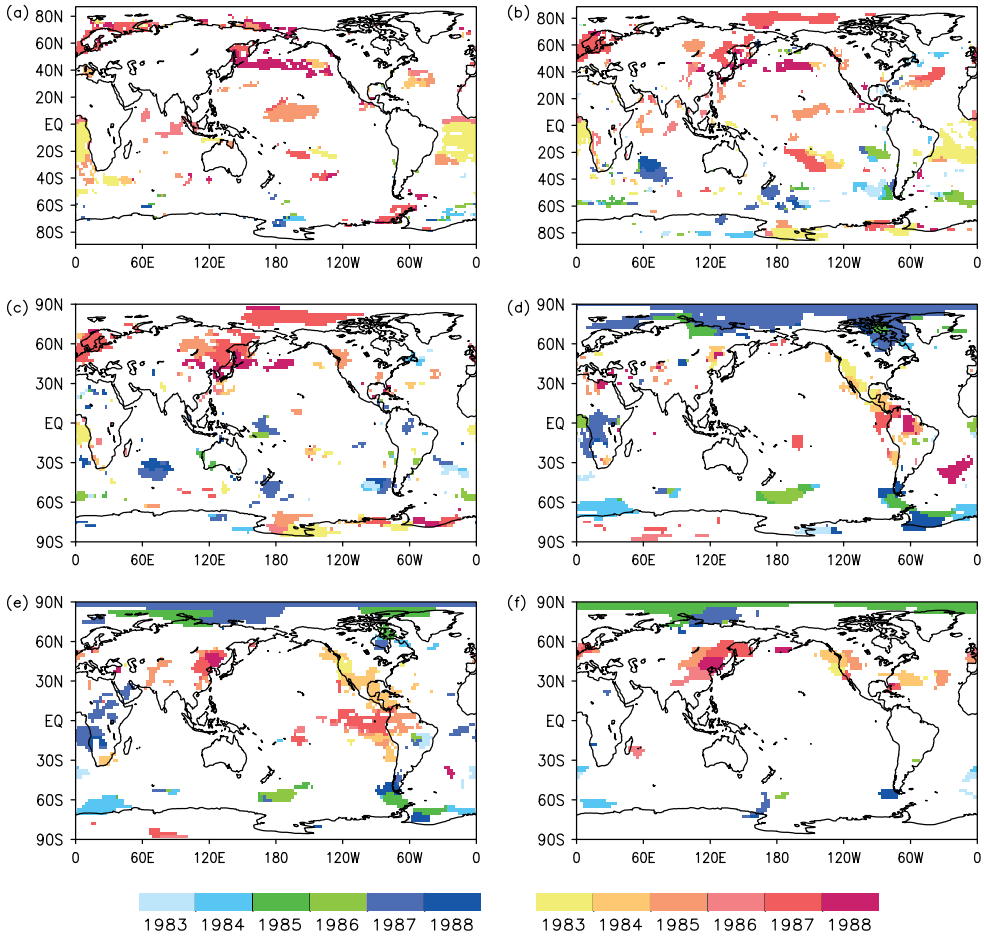

Figure 1. Horizontal distributions of the DACYs in the 1980s of annual averaged variables (a) SST, (b)ULWRF, (c) SAT, (d) SLP, (e) 850-hPa and (f) 500-hPa geopotential height. The cold colour scheme (green, blue, etc.) and warm colour scheme (yellow, red, etc.) represent the decreased DACYs and increased DACYs significant at the 95% confidence level, respectively. The false discovery rate of the DACYs in each field is controlled at 0.05. This figure is available in colour online at wileyonlinelibrary.com/journal/joc

the Arctic occurred in 1985 and 1987, respectively. In Figure 2(a), there were significant negative anomalies of 500-hPa geopotential height over the Arctic with a minimum value about −35 geopotential meter (gpm), accompanied with zonal midlatitude positive anomalies, significantly over west Europe, northeast Asia, Canada, and subtropical Atlantic, with the maximum values about 15–20 gpm. In Figure 2(b), anomalous winds went out from the Arctic column and anomalous anticyclones occupied the above four regions with positive geopotential height. The westerly anomalies over the North Pacific and North Atlantic indicated the weaker Pacific and Atlantic subtropical jets, which is consistent with that of the findings of Watanabe and Nitta (1998, 1999). The structures of 500-hPa geopotential height, as decrease over the Arctic and increase over the NH midlatitudes, presented a meridional see-saw structure, which is similar to that of the NAM introduced by Thompson and Wallace (1998) and Li and Wang (2003). The relationship between the atmospheric DACs in the 1980s and the NAM DAC will be discussed in section 4.

Figure 2(c) and 2(d) display the epoch difference of 850-hPa air temperature and horizontal winds anomalies, respectively. The significant positive anomalies of 850-hPa air temperature and horizontal winds are analogous to that of the 500-hPa geopotential height. It shows a warmer air temperature over west Europe, northeast Asia, west Canada, and subtropical Atlantic. The meridional gradient of 850-hPa air temperature between midlatitude and Arctic increased after 1987 because of positive air temperature anomalies over the midlatitude and negative ones in the high latitude.

3.2. Temporal variations of the DACYs in the 1980s

In order to confirm the authenticity of the DACs in the 1980s, several time series are shown in Figure 3, which are selected according to the DAC regions in Figure 1. The IDACs of SST over the southern tropical Atlantic (Figure 3(a)) occurred in 1983, with an enhancement 0.43 °C of mean value. A DDAC and an IDAC of SST over the northern North Pacific (Figure 3(b)) took place in 1975 and 1988, with a decrease of 0.44 °C and an increase 0.49 °C of mean values, respectively. The IDACs of SAT over northeast Asia (Figure 3(c)) and north Europe (Figure 3(d)) happened simultaneously in 1987, with enhancement of 0.62 °C and 0.78 °C in mean values, respectively. Figure 3(e) exhibits the IDAC of 500-hPa geopotential height of west Canada occurred in

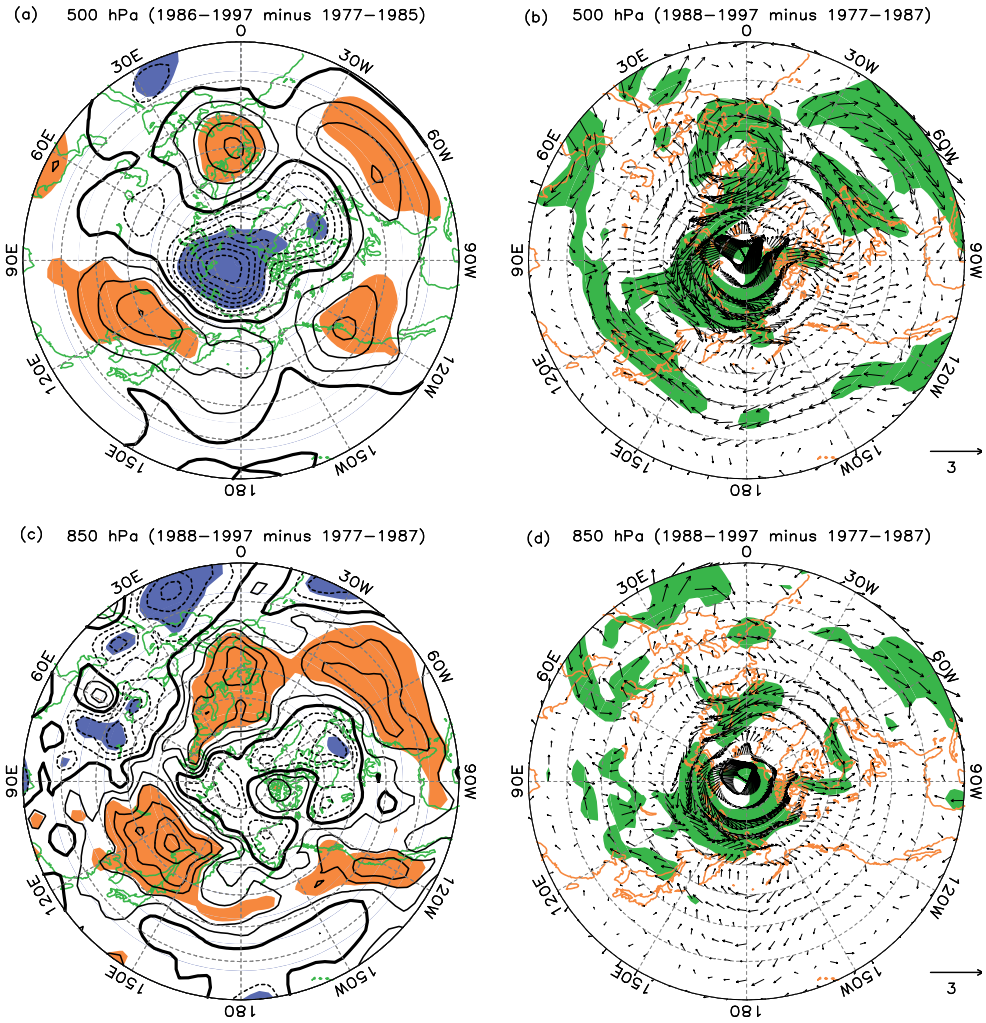

Figure 2. Epoch difference maps of 500-hPa (a) geopotential height and (b) horizontal winds and 850-hPa (c) air temperature and (d) horizontal winds for forward-minus-later annual mean (years as indicated above each panel), respectively. The colour-shaded domains in (a) and (c) are significant at the 95% confidence level based on Student's t-test. The black contour intervals are 5 gpm in (a) and 0.2 °C in (c), respectively. Negative contours are dashed; and the zero contours are thickened. The colour shaded domains in (b) and (d) represent the 90% confidence levels of horizontal winds according to vector Student's t-test. This figure is available in colour online at wileyonlinelibrary.com/journal/joc

1984. The mean value of the period after 1984 increased 16.42 gpm than that of the period before then. According to the above time series, it is obvious that the DACs of the ocean–atmosphere system in the 1980s are actually existent. Moreover, the DACYs of different regions and different levels were asynchronous.

Figure 4 displays the time series of the meridional differences (subtracting the Arctic air temperature anomalies from midlatitudes') of 850-hpa, 500-hPa, and 200-hpa air temperature anomalies between the middle and high latitudes. The IDAC and DDAC of the meridional difference at 850-hPa between the northern midlatitude and Arctic happened in 1985 and 2004 (Figure 4(a)). The mean values of the northern meridional difference increased 0.46 °C and decreased 0.56 °C, respectively. There are two decreased DACYs in 1975 and 1994 and an increased DACY in 1985 in the time series of the meridional difference of 500-hpa air temperature anomalies between the midlatitude and Arctic (Figure 4(b)). An IDAC and a DDAC occurred in the 1987 and 1997 in the time series of the meridional difference of 200-hpa air temperature anomalies between the NH middle and high latitudes, respectively (Figure 4(c)). The above facts suggested an enhanced meridional gradient of tropospheric air temperature anomalies between the NH midlatitudes and Arctic.

3.3. Vertical distributions of the DACYs in the 1980s

Figure 5 indicates the vertical structures of the DACs of geopotential height and horizontal winds. Figure 5(a) shows that the DDACs of the Arctic geopotential height occurred at 700–300-hPa in 1985, at 1000–850-hPa and 200–10-hPa in 1987, and its IDACs happened at 1000–20-hPa in 1997. The DDACs at 700–300-hPa of the Arctic geopotential height in the 1980s were 2 years in advance of that at the others levels. It can be seen that the DACs in the 1980s happened at not only one level but almost all levels. Figure 5(b) – (h) show that the DACs of the zonal wind around the midlatitude anomalous anticyclones happened in the 1980s. These

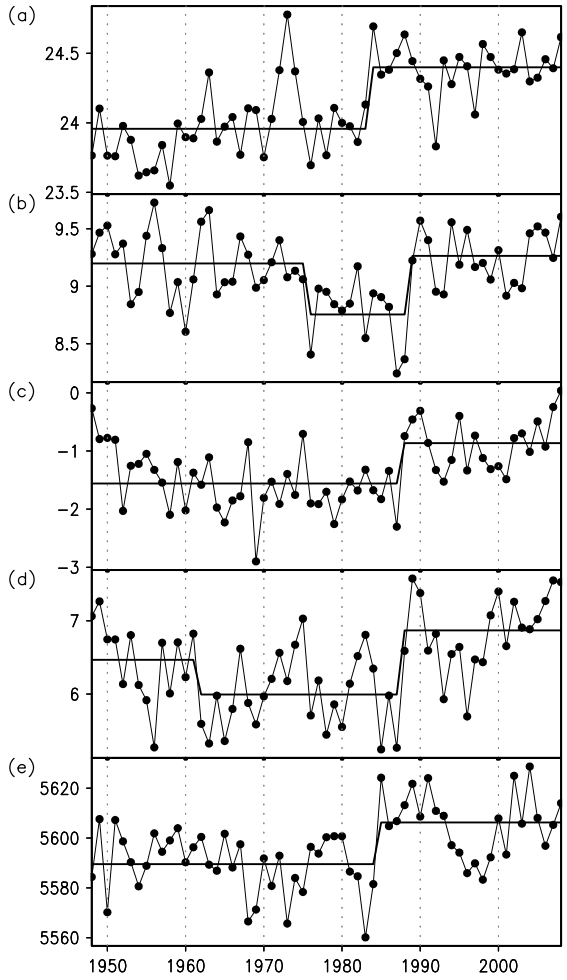

Figure 3. Annual averaged time series (dotted solid line, 1948–2008) and epoch average (thick solid line) of the regions (a) SST (0 °S–25 °S, 30 °W–15 °E) (unit: °C), (b) SST (40°N–50°N, 140 °E–150 °W) (unit: °C), (c) SAT (40°N–70°N, 120 °E–160 °E) (unit: °C), (d) SAT (45°N–70°N, 5 °W–40 °E) (unit: °C), and (e) 500-hPa geopotential height (42.5 °N–52.5 °N, 140 °W–120 °W) (unit: gpm). The epoch averages are divided by the DACYs significant at the 95% confidence level.

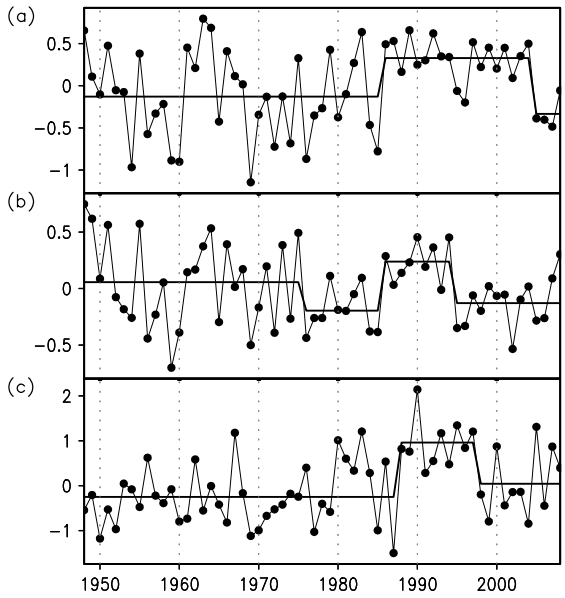

Figure 4. Same as Figure 3, but for the difference of zonal mean air temperature anomalies between (a) 40°N–65°N and 70°N–90°N at 850 hPa, (b) 30°N–65°N and 70°N–90°N at 500 hPa, and (c) 30°N–50°N and 55°N–90°N at 200 hPa. The first DACY in Figure 4(b) is significant at 90% confidence level.

facts confirmed the NH midlatitude anomalous anticyclones. The DDACs and IDACs of the NH circumpolar zonal winds (Figure 5(i)) occurred at all levels in 1987 and 1997, respectively. It means that the westerly anomalies occupied the northern circumpolar regions at all levels since the late 1980s. The above vertical structures (Figure 5(a)–(i)) are suggestive of an equivalent barotropic structure of the NH atmospheric DACs in the 1980s. Figure 5(j) indicates that the IDACs of the NH circumpolar meridional wind occurred at 1000–925-hPa in 1987, and its DDACs occurred at 700–100-hPa in 1987–1988. The facts indicated that anomalous meridional winds went into (out from) the Arctic column at the lower (middle and high) troposphere. It is interesting whether there is a decadal anomalous vertical circulation across the NH extratropics which charges the atmospheric mass exchanges between the midlatitude and Arctic.

4. Decadal anomalies of atmospheric mass exchanges between the NH middle and high latitudes

The NAM represents the atmospheric mass fluctuations between the NH middle and high latitudes (Thompson and Wallace, 1998; Li and Wang, 2003). As has been noted, there were decadal anomalies of atmospheric mass exchanges between the NH middle and high latitudes since the late 1980s. For a further investigation, the following questions associated with the atmospheric mass exchange between the NH middle and high latitudes and the NAM are taken up.

Is the NH midlatitude the corresponding region of increase mass that must accompany a removal of mass from the Arctic atmosphere?

In order to understand whether decadal anomalies of the atmospheric mass exchanges exist between the Arctic and the NH midlatitude, Figure 6 displays the epoch differences of the meridional-height cross-sections of winds field. Figure 6(a) displays that the anomalous airflows arose over the Arctic, moved southward and descended over the 40°N–50°N belt (corresponding to west Canada). Figure 6(b) shows that the winds anomalies ascended over the 50°N–70°N belt and moved northward and partly downward at 80°N, and another air current moved southward and descended over the 20°N–40°N belt (corresponding to the subtropical Atlantic). Figure 6(c) indicates that the anomalous winds went upward over the 60°N–70°N belt. One air current went northward at higher levels, and another went southward and descended at 45°N–60°N belt (corresponding to the West Europe). In Figure 6(d), there are upward airflows over the 75°N–90°N belt and downward airflows over the 45°N–70°N belt (corresponding to the northeast Asian).

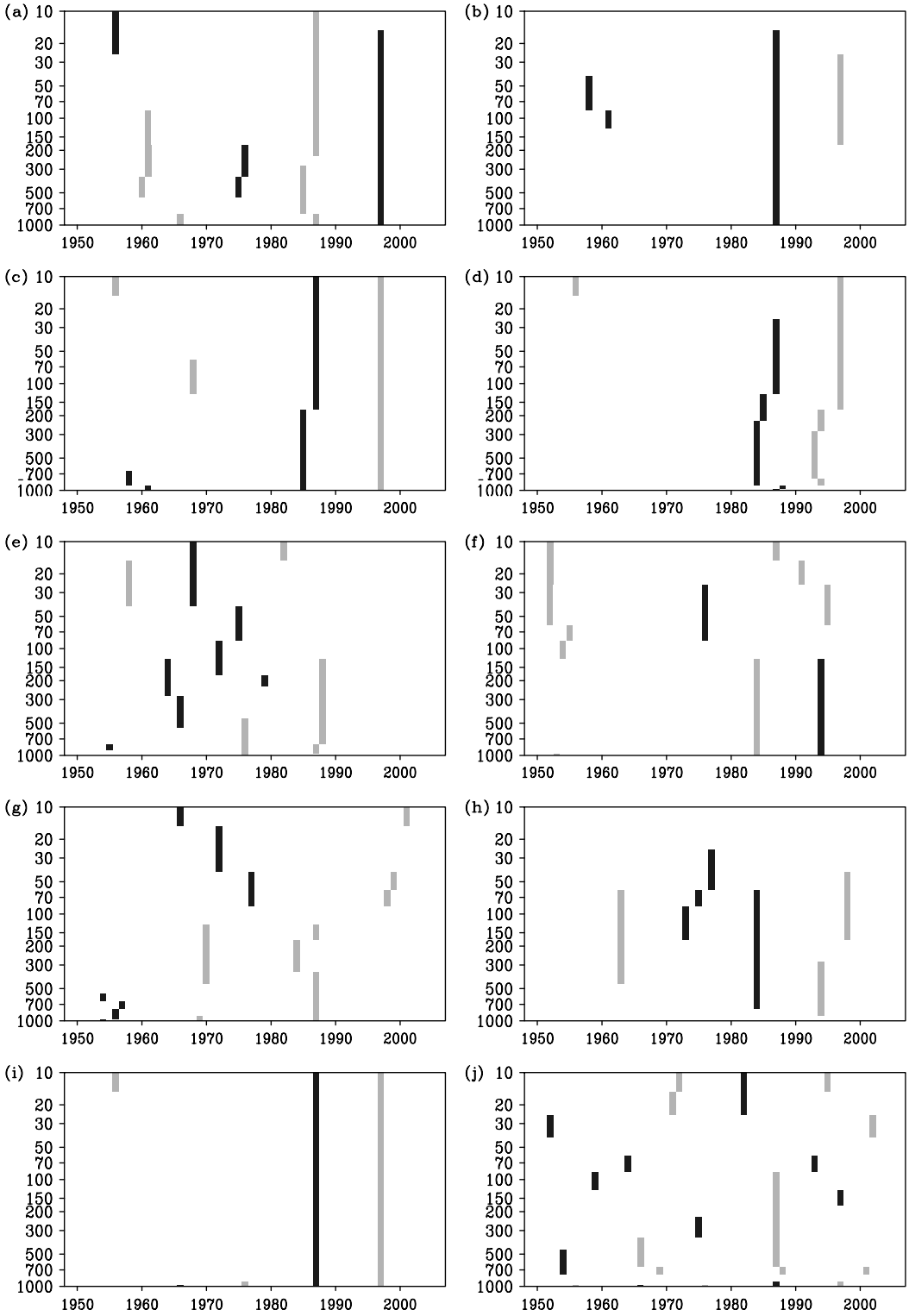

Figure 5. Vertical distributions of the DACYs of annual averaged geopotential height over (a) (80°N–90°N, 0°E–357.5°E), annual averaged zonal winds over (b) (60°N–75°N, 0°E–30°E), (c) (60°N–70°N, 90°E–150°E), (d) (60°N–75°N, 140°W–100°W), (e) (30°N–40°N, 100°E–120°E), (f) (35°N–45°N, 150°W–120°W), (g) (17.5°N–27.5°N, 75°W–45°W), (h) (40°N–50°N, 60°W–30°W) and (i) (60°N–75°N, 0°E–357.5°E), and annual averaged meridional wind over (j) (60°N–75°N, 0°E–357.5°E). The dark and light shading refer to the increased DACYs and decreased DACYs significant at the 95% confidence level, respectively. The false discovery rate of the DACYs in each field is controlled at 0.05.

Moreover, another air current from subtropics descended here. Compared with Figure 2(c) and Figure 6, it can be seen that the domains of the descending airflows are corresponding to that with decadal positive anomalies of 500-hPa geopotential height and 850-hPa air temperature. Therefore, the warming of the NH midlatitude domains may be attributed to the dropping currents from the Arctic. Furthermore, Figure 7 indicates that there was an

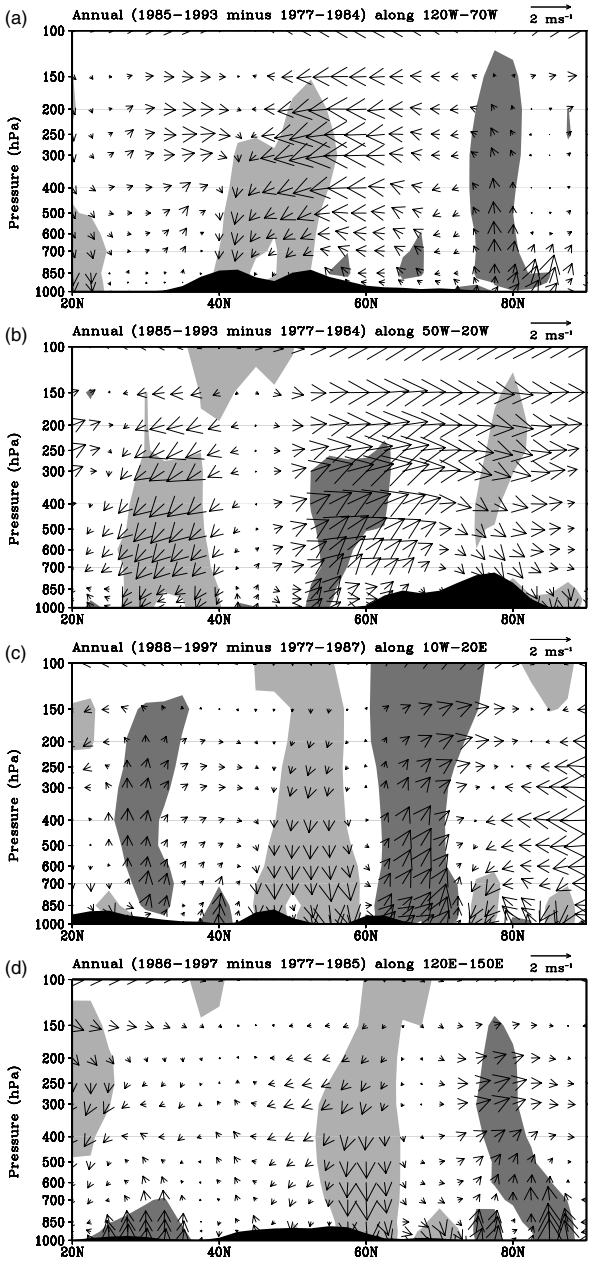

Figure 6. Epoch difference maps of meridional-height cross-section of wind changes along (a) (120 °W–70 °W), (b) (50 °W–20 °W), (c) (10 °W–20 °E), and (d) (120 °E–150 °E) for forward-minus-later annual mean (years as indicated above each panel), respectively. The lighter and darker shaded domains represent the downward and upward vertical anomalies significant at 95% confidence level based on Student's *t*-test, respectively. The black shading denotes the topography.

anomalous vertical circulation over the northern extratropics with Arctic upward airflows and midlatitudinal downward airflows. It is obvious that the NH midlatitude is the corresponding region of increase mass that associated the shift of mass from the Arctic atmosphere.

Are the decadal anomalies of the northern extratropical atmospheric mass exchanges demonstrated the NAM DAC in the 1980s?

Li and Wang (2003) pointed out that the positive NAM phase is essentially the result of the anomalous Ferrel

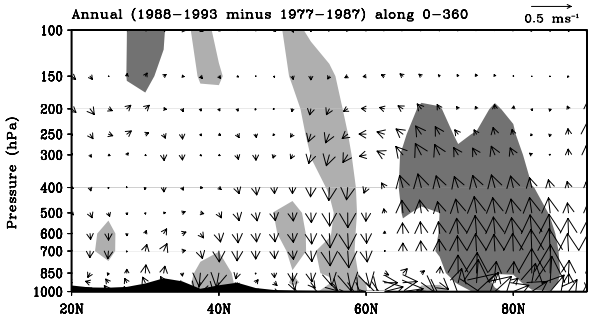

Figure 7. Same as Figure 6, but for the zonal averaged wind anomalies.

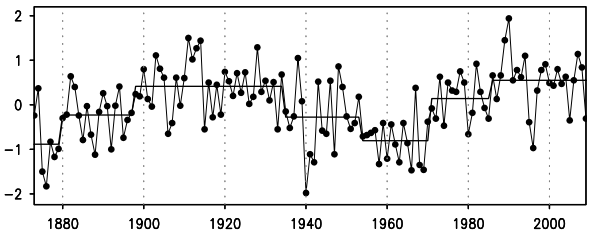

Figure 8. Same as Figure 3, but for the annual NAM index (1873–2009).

cell. Figure 7 indicated that a vertical current circulation located over the NH extratropics, with the upward (downward) wind anomalies over the Arctic (NH midlatitude). Another air current from the northern subtropics descended over the middle latitudes. This structure indicated apropos the anomalies of the Ferrel cell. Therefore, the decadal anomalies of the northern extratropical atmospheric mass exchanges testified the NAM DAC in the 1980s. Moreover, there are several witnesses considered as the supplementary for indentifying the NAM DAC in the 1980s. As presented in Section 3, the anomalies of the northern extratropical 500-hPa geopotential height and 850-hPa air temperature presented a meridional see-saw structure, so did that at the others levels. The DACs of the Arctic and NH midlatitude geopotential height and air temperature indicated an equivalent barotropic structure. Such meridional see-saw and equivalent barotropic structures in the northern extratropical atmosphere are the most important features of the NAM. What is more, Figure 8 also showed an abrupt increase of the NAM index in 1985. Furthermore, the DACs of NAM also occurred in 1897, 1934, 1953, and 1969. In regards to the decadal anomalous structures of the NAM, the above findings, including the decadal anomalies of the Ferrel cell, the meridional see-saw structures, an equivalent barotropic structure and the NAM index, suggest that the NAM DAC in 1985 is a part of the DAC event in the 1980s.

5. Discussion

The horizontal, vertical, and temporal structures of the DACs of the northern extratropical ocean–atmosphere system in the 1980s have been shown above. The decadal

changes of the meridional atmospheric mass exchanges also were discussed. In this section, the possible physical process, which was implicated in the spatial and temporal structures of the DACs in the 1980s, and the meridional atmospheric mass exchanges, is proposed and used to explain the associated climate change events in northern extratropics.

What is the explanation for the decadal anomalies of the meridional atmospheric mass exchanges between the NH middle and high latitudes, namely, the possible physical process of the DACs in the 1980s?

According to the facts noted in this study, the possible physical process of the DACs in the 1980s could be proposed as follows. The IDACs of the northern midlatitude SST heated the local atmosphere and it caused the decadal anomalies of the meridional air temperature gradient between middle and high latitudes. Decadal anomalies of the Ferrel cell, namely, the decadal anomalies of meridional atmospheric mass exchanges between the NH midlatitude and Arctic were triggered by the force of the meridional gradient of the air temperature.

The detailed physical process of the DACs of the northern extratropical ocean–atmosphere system in the 1980s may be formed as shown in Figure 9. The IDACs of SST over the northern midlatitude occurred in 1984–1988. The distribution of the DACs of ULWRF is similar to that of SST in the NH midlatitude (Figure 1(a) and (b)) which indicated the decadal increase of oceanic heating. The decadal warming of NH midlatitude SST heated the lower tropospheric atmosphere. What accompany it was the increased air temperature meridional gradient between the NH middle latitudes and the Arctic at lower levels (Figure 4(a)). In the light of the geostrophic wind principle, the westerly wind anomalies prevailed over the circumpolar region in the lower troposphere. In the lower troposphere, the westerly wind anomalies deflected and went into the Arctic because of the topographical frictional action. It can be seen in Figure 5(j) that the IDACs of meridional winds occurred over the NH circumpolar region at 1000–925-hPa in 1987 which indicated decadal anomalies of meridional winds around the Arctic. At the middle and high troposphere, the upward airflow over the Arctic diverged (Figure 7) and the southward currents deflected right over the NH midlatitude under the action of the geostrophic deflection force formed the anticyclonic anomalies and descended in the NH midlatitude nearby the regions of warming SST. Furthermore, the dynamical warming effect of the downward airflows heated the middle and high tropospheric atmosphere. Hence, the IDACs of the NH midlatitude SST may lead to the decadal anomalies of Ferrel cells with the result of the Arctic DDACs, the NH midlatitude IDACs of geopotential height and the NAM DAC in the 1980s.

The physical process proposed above is not consistent with all the timing order of the DACs of different levels. For instance, it can be seen in Figures 2 and 5(a) that the DACs of 850-hPa and 500-hPa Arctic geopotential height occurred in 1987 and 1985, respectively. This situation may be attributed to two situations as follows. On the one

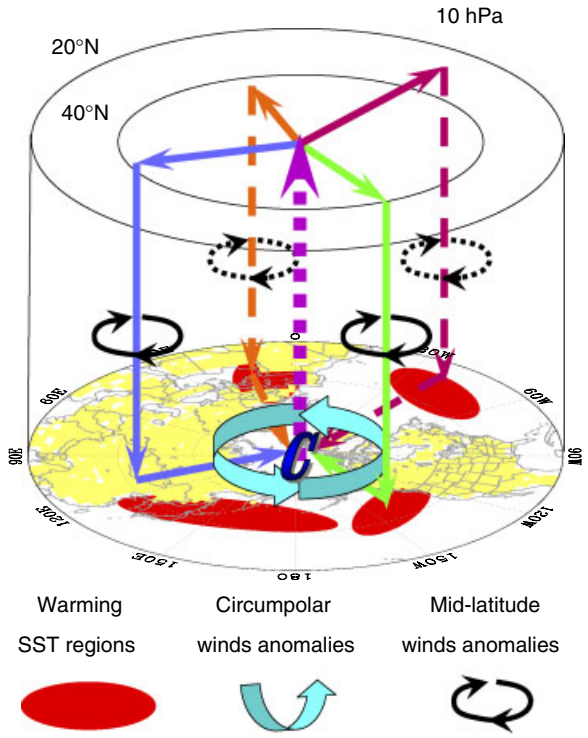

Figure 9. Schematic diagram showing the possible physical process of the DACs of the northern extratropical ocean–atmosphere system in the 1980s. The red regions represent the warming SST domains; the black arrows denote the midlatitude anticyclones; the tridimensional colour arrows represent the circumpolar anomalous winds; the coloured arrows stand for the motion of the air current; and the letter 'C' denotes the cyclone. This figure is available in colour online at wileyonlinelibrary.com/journal/joc

hand, the values of 850-hPa and 200-hPa geopotential height of 1987 are higher than the mean value of the epoch before 1987, neither does the value of 500-hPa geopotential height of 1987 (Figure 10). The above fact is why the occurrence time of the DACs of 500-hPa and 850-hPa geopotential height is inconsistent. If the values of 500-hPa geopotential height are equal to or higher than the mean value of the period 1976–1985 of 500-hPa Arctic geopotential height, the DACY of 500-hPa geopotential height is 1987, which is consistent of the DACY of 850-hPa and 200-hPa geopotential height. Therefore, the difference between the DACYs of 850-hPa and 500-hPa geopotential height may be attributed to the error of the 500-hPa geopotential height of 1987. The timing consistency of the DACs of ocean–atmosphere system in the 1980s should be satisfied in the condition of the precise reanalysis data on every grid. However, it is impossible to ensure that the reanalysis data on every grid is exact. Generally, the difference of the DACY in 1–2 years is receivable, which may be due to the error of reanalysis data. On the other hand, the reanalysis data of 500 hPa geopotential height on every grid is exact. For example, the Arctic DACs of 500-hPa geopotential height in 1985 may be related to the transport from the west coast of Canada whose DACs occurred in 1984. However, it is hard to be illustrated to this extent. On the while, the timing of the DACYs in

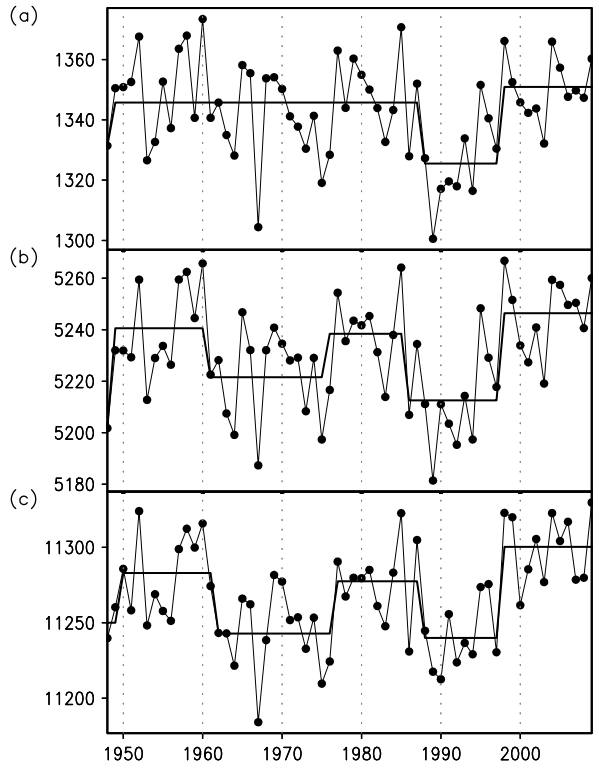

Figure 10. Same as Figure 3, but for geopotential height over the regions (0 °E–357.5 °E, 80°N–90°N) (a) at 850-hPa, (b) at 500 hPa, and (b) at 200 hPa (unit: gpm).

the 1980s of the northern extratropical ocean–atmosphere system is consistent of the physical process proposed in the manuscript.

How do we understand the NH extratropical climate changes from the view of the above physical process of the DACs in the 1980s?

Figure 1(c) and 2(c) show the warming regions over west Europe, northeast Asia, west Canada, and subtropical Atlantic. From the view of this study, the decadal warming of the above regions was attributed to the joint actions of the heating of SST and the dynamical warming effects of the dropping airflows above them. Besides the warming events indicated in this study, several climate change events are coincident with the DACs in the 1980s. The summer precipitation (air temperature) over northeast (northwest) China decreased (increased) since the middle 1980s (Wu *et al*., 2008). The dropping airflows over northeast Asia are conducive to a decrease in precipitation and the increase of the air temperature over northeast China. The increase of precipitation over northwest China (Shi *et al*., 2002) benefited from the decadal anomalous upward airflows there (not shown). The East Asian winter monsoon index tended to be weaker since the mid-1980s (Youn, 2005). The occurrence number of the spring dust storms over northwest China became less than before since the late 1980s (Ding *et al*., 2005; Liu and Ding, 2007; Zhu *et al*., 2008). Because of the anomalous anticyclone over northeast Asia, there were northeasterly and southeasterly wind anomalies over northeast and northwest China, respectively. Regarding the winds anomalies, such anomalous circulations are instrumental in the weakening of the East Asian winter monsoon and the decrease of the spring dust storms. Furthermore, the global hurricane number (including the storms of intensity >33 m s^{-1}) and hurricane days were decadal in increase in 1988–1997 (Webster *et al*., 2005). Figure 5(a) shows that the Arctic geopotential height was in a decadal anomalous positive phase in 1988–1997. It is interesting that whether there is a relationship between the global hurricane number and hurricane days and the Arctic vortex on decadal time scale. It needs further study.

Sea ice is an important indicator of changes in the climate system. The SLP and wind anomalies over the Arctic could affect the Arctic sea ice extent and concentration (Wu *et al*., 2004). As has been noted, the anomalies of the meridional wind of the NH circumpolar went northward to the Arctic at the lower troposphere. The northward meridional winds at the lower levels brought the warmer air into the Arctic, which is conducive to the decrease of the Arctic sea ice, especially the inshore thin sea ice. It may be the thermal cause of the decrease of the summer sea ice in the offshore region of Siberia (Maslanik *et al*., 1996) and the southern Okhotsk Sea (Tachibana *et al*., 1996).

6. Summary and conclusion

The horizontal, vertical, and temporal structures, meridional atmospheric mass exchanges and the physical process of the northern extratropical DACs in the 1980s are discussed in this study. The IDACs of SST happened over the northern North Pacific, middle Pacific, southern tropical Atlantic and northern North Atlantic in 1983–1988. The characteristics of atmospheric DACs in 1983–1988 were displayed in terms of changes of higher air temperature and geopotential height over northeast Asia, west Europe, northern subtropical Atlantic and west Canada, and lower over the Arctic. These findings identified that the northern extratropical DACs in the 1980s are facts. The decadal anomalies of the meridional circulations indicated that the midlatitude increase of mass is a removal of the Arctic atmospheric mass. Furthermore, the meridional circulation between the middle and high latitudes indicated the decadal anomalies of the Ferrel cell. The IDAC of NAM in 1985 was addressed with the NAM index and a decadal positive phase of the Ferrel cell.

The possible physical process of the DACs in the northern extratropical ocean–atmosphere system in the 1980s is proposed as follows. The IDACs of northern midlatitude SST heated the local lower atmosphere. As a result, the meridional gradient of air temperature between the middle latitudes and Arctic increased abruptly at lower levels. The anomalous geostrophic westerly winds, which paralleled the geographic parallel, prevailed over the circumpolar region at the lower levels. In the lower troposphere, the westerly wind anomalies deflected and

went into the Arctic because of the topographical frictional action. In the middle and high troposphere, the upward airflow over the Arctic diverged and the southward currents deflected right over the NH midlatitude under the action of the geostrophic deflection force, formed the anticyclonic anomalies and descended near the regions of warming SST in the NH midlatitude. Meanwhile, a decadal anomalous Ferrel cell established over the northern extratropics. An access of decadal atmospheric mass exchange between the middle latitudes and Arctic was established. The downward airflows of anomalous Ferrel cell heated the tropospheric midlatitude atmosphere whose areas were located near the regions of warming SST. Therefore, the IDACs of NH midlatitude SST were the possible origin of the DACs of the northern extratropical ocean–atmosphere system in the 1980s. Furthermore, the physical process of the DACs of the northern extratropical ocean–atmosphere system in the 1980s proposed in this study could well explain the decadal warming of the NH continent, weakening of East Asian winter monsoon, decreasing (increasing) of the precipitation (air temperature) over northeast China, and the less frequent occurrence of the spring dust storm over northwest China, as well as the NAM DAC in the mid-1980s.

Acknowledgments

Our thanks to B. Wu, J. Wang, J. Feng, W. Zhang, and L. Feng for their help. This work was jointly supported by the National Basic Research Program (2010CB950400), Natural Science Foundation of China (40890050, 40528006 and 90711003).

References

Angell JK. 2006. Changes in the 300-mb North Circumpolar Vortex, 1963-2001. *Journal of Climate* **19**: 2984–2994.

Benjamini Y, Hochberg Y. 1995. Controlling the false discovery rate: A practical and powerful approach to multiple testing. *Journal of the Royal Statistical Society B* **57**(1): 289–300.

Deser C, Blackman ML. 1993. Surface Climate Variations over the North Atlantic Ocean during Winter: 1900–1989. *Journal of Climate* **6**: 1143–1153.

Deser C, Phillips AS, Hurrell JW. 2004. Pacific interdecadal climate variability: linkages between the Tropics and the North Pacific during boreal winter since 1900. *Journal of Climate* **17**: 3109–3124.

Ding RQ, Li JP, Wang SG, Ren FM. 2005. Decadal change of the spring dust storm in northwest China and the associated atmospheric circulation. *Geophysical Research Letters* **32**: L02808, DOI:10.1029/2004GL021561.

Graham NE. 1994. Decadal-scale climate variability in the tropical and North Pacific during the 1970s and 1980s: observations and model results. *Climate Dynamics* **10**: 135–162.

Hare SR, Mantua NJ. 2000. Empirical evidence for North Pacific regime shifts in 1977 and 1989. *Progress in Oceanography* **47**: 103–145.

Huang JY. 2000. *Statistic analysis and forecast methods in meteorology*. China Meteorology Press: Beijing; pp. 25–27.

Jiang JM, You XT. 1996. Where and when did an abrupt climatic change occur in China during the last 43 years? *Theoretical and Applied Climatology* **55**: 33–40.

Jiang JM, Fraedrich K, Zou YR. 2001. A scanning t-test of multiscale abrupt changes and its coherence analysis. *Chinese Journal of Geophysics* **44**(1): 31–39.

Kalnay EM, Kanamitsu M, Kistler R, Collins W, Deaven D, Gandin L, Iredell M, Saha S, White G, Woollen J, Zhu Y, Chelliah M, Ebisuzaki W, Higgns W, Janowiak J, Mo KC, Ropelewski C, Wang J, Leetmaa A, Reynolds R, Jenne R, Joseph D. 1996. The NCEP/NCAR reanalysis project. *Bulletin of the American Meteorology Society* **77**: 437–471.

Kushnir Y. 1994. Interdecadal variations in the North Atlantic sea-surface temperature and associated atmospheric conditions. *Journal of Climate* **7**: 141–157.

Latif M, Barnett TP. 1994. Causes of decadal climate variability over the North Pacific and North America. *Science* **266**: 634–637.

Li JP, Wang JX. 2003. A modified zonal index and its physical sense. *Geophysical Research Letters* **30**(12): 1632, DOI:10.1029/2003GL0177441.

Liu XH, Ding RQ. 2007. The relationship between the spring Asian atmospheric circulation and the previous winter Northern Hemisphere annular mode. *Theoretical and Applied Climatology* **88**: 71–81.

Lo TT, Hsu HH. 2010. Change in the dominant decadal patterns and the late 1980s abrupt warming in the extratropical Northern Hemisphere. *Atmospheric Science letters* **11**: 210–215.

Mantua NJ, Hare SR, Zhang Y, Wallace JM, Francis RC. 1997. A Pacific interdecadal climate oscillation with impacts on salmon production. *Bulletin of the American Meteorology Society* **78**: 1069–1079.

Martinson DG, Bryan K, Ghil M, Karl TR, Sarachik ES, Sorooshian S, Talley LD. 1995. *Natural Climate Variability on Decade-to-Century Time Series. Introduction*. National Academy Press: Washington, DC; pp. 5–8.

Maslanik JA, Serreze MC, Barry RG. 1996. Recent decreases in Arctic summer ice cover and linkages to atmospheric circulation anomalies. *Geophysical Research Letters* **23**: 1677–1680.

Mehta V, Lindstrom E, Busalacchi A, Delworth T, Deser C, Fu LL, Hansen J, Lagerloef G, Lau K-M, Levitus S, Meehl G, Mitchum G, Sarachik E, Susskind J, White W. 2000. Proceedings of the NASA workshop on decadal climate variability. *Bulletin of the American Meteorology Society* **81**(12): 2983–2985.

Nitta T, Yamada S. 1989. Recent warming of tropical sea surface temperature and its relationship to the Northern Hemisphere circulation. *Journal of the Meteorology Society of Japan* **67**: 375–383.

Overland JE, Spillane MC, Percival DB, Wang MY, Mofjeld HO. 2004. Seasonal and regional variation of Pan-Arctic surface air temperature over the instrumental record. *Journal of Climate* **17**: 3263–3282.

Schwing FB, Jiang J, Mendelssohn R. 2003. Coherency of multi-scale abrupt changes between the NAO, NPI, and PDO. *Geophysical Research Letters* **30**(7): 591–594.

Shi YF, Shen YP, Hu RJ. 2002. Preliminary Study on Signal, Impact and Foreground of Climatic Shift from Warm-Dry to Warm-Humid in Northwest China. *Journal of Glaciology and Geocryology* **24**: 119–226.

Smith TM, Reynolds RW. 2004. Improved extended reconstruction of SST (1854-1997). *Journal of Climate* **17**: 2466–2477.

Tachibana Y, Honda M, Takeuchi K. 1996. The abrupt decrease of the sea ice over the southern part of the sea of Okhotsk in 1989 and its relation to the recent weakening of the Aleutian low. *Journal of the Meteorology Society of Japan* **74**: 579–584.

Thompson DJ, Wallace JM. 1998. The Arctic Oscillation signature in the wintertime geopotential height and temperature fields. *Geophysical Research Letters* **25**: 1297–1300.

Ting M, Hoerling MP, Xu T, Kumar A. 1996. Northern hemisphere teleconnection patterns during extreme phases of zonal-mean circulation. *Journal of Climate* **9**: 2614–2633.

Trenberth KE. 1990. Recent observed interdecadal climate changes in the Northern Hemisphere. *Bulletin of the American Meteorology Society* **71**: 988–993.

Trenberth KE, Hurrell JW. 1994. Decadal atmospheric-ocean variations in the Pacific. *Climate Dynamics* **9**: 303–319.

Wallace JM. 2000. North Atlantic Oscillation per annular mode: Two paradigms, one phenomenon. *Quarterly Journal of the Royal Meteorological Society* **126**: 791–805.

Walsh JE, Chapman WL, Shy TL. 1996. Recent decrease of the sea level pressure in central Arctic. *Journal of Climate* **9**: 480–486.

Watanabe M, Nitta T. 1998. Relative impacts of snow and sea surface temperature anomalies on an extreme phase in the winter atmospheric circulation. *Journal of Climate* **11**: 2837–2857.

Watanabe M, Nitta T. 1999. Decadal changes in the atmospheric circulation and associated surface climate variations in the Northern Hemisphere winter. *Journal of Climate* **12**: 494–510.

Webster PJ, Holloand GL, Curry JA, Chang H-R. 2005. Changes in tropical cyclone number, duration, and intensity in a warming environment. *Science* **309**: 1844–1846.

Wu BY, Wang J, Walsh JE. 2004. Possible Feedback of Winter Sea Ice in the Greenland and Barents Seas on the Local Atmosphere. *Monthly Weather Review* **132**: 1868–1876.

Wu BY, Zhang RH, D'Arrigo R. 2008. Arctic dipole anomaly and summer rainfall in Northeast China. *Chinese Science Bulletin* **53**: 2222–2229.

Xiao D, Li JP. 2007a. Spatial and temporal characteristics of the decadal abrupt changes of atmosphere-ocean system in 1970s. *Journal of Geophysical Research* **112**: D24S22, DOI:10.1029/2007 JD008956.

Xiao D, Li JP. 2007b. Main decadal abrupt changes and decadal modes in global sea surface temperature field (in Chinese). *Journal of Atmospheic Science* **31**(5): 839–854.

Youn Y-H. 2005. The climate variabilities of air temperature around the Korean peninsula. *Advances in Atmospheric Science* **22**: 575–584.

Yu RC, Zhou TJ. 2007. Seasonality and three-dimensional structure of the interdecadal change in East Asian monsoon. *Journal of Climate* **20**: 5344–5355.

Zhang Y, Wallace JM, Battisti DS. 1997. ENSO-like interdecadal variability: 1900–93. *Journal of Climate* **10**: 1004–1020.

Zhu CW, Wang B, Qian WH. 2008. Why do dust storms decrease in northern China concurrently with the recent global warming? *Geophysical Research Letters* **35**: L18702, DOI:10.10292008GL034886.

